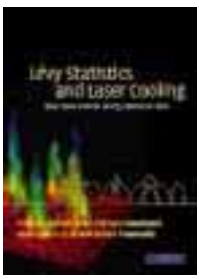

Lévy Statistics and Laser Cooling

How Rare Events Bring Atoms to Rest

François Bardou, Jean-Philippe Bouchaud, Alain Aspect, Claude Cohen-Tannoudji

Book DOI: http://dx.doi.org/10.1017/CBO9780511755668

Online ISBN: 9780511755668

Hardback ISBN: 9780521808217

Paperback ISBN: 9780521004220

Chapter

6 - The momentum distribution pp. 69-87

Chapter DOI: http://dx.doi.org/10.1017/CBO9780511755668.007

Cambridge University Press

6

The momentum distribution

The fraction of *trapped* atoms $f_{\text{trap}}(\theta)$ studied in Chapter 5 gives global information on the efficiency of subrecoil laser cooling: the proportion of atoms accumulated within the sphere of radius p_{trap}. Within this sphere, one expects the momentum distribution to exhibit a narrow peak, containing the *cooled* atoms. Knowledge of $f_{\text{trap}}(\theta)$ does not provide enough information about this peak: for instance, one might trap a significant fraction of atoms within p_{trap} but, in some unfavourable cases, these atoms could be somewhat uniformly distributed over the trap, leaving only a negligible fraction in the peak itself.

In order to get a better characterization of the cooling, we calculate in this chapter the momentum distribution $\mathcal{P}(\mathbf{p})$ of the atoms contained within the sphere of radius p_{trap}. In particular, we derive analytical expressions for various important features of the narrow peak of $\mathcal{P}(\mathbf{p})$: its half-width $w(\theta)$; its height $h(\theta)$; its weight $f_{\text{peak}}(\theta)$ (which we will call the 'cooled fraction'); the shape of its tails and of its central part. We also estimate the phase space density increase associated with the cooling process. This will enable us to identify the relevant physical parameters of subrecoil cooling and to get a better understanding of the role of non-ergodicity.

6.1 Brief survey of previous heuristic arguments

Before using the statistical tools introduced in Chapter 4, which will prove to be very efficient for investigating the momentum distribution $\mathcal{P}(\mathbf{p})$, it is useful to come back to the heuristic arguments which were first used [AAK88] to estimate certain physical quantities such as the half-width $w(\theta)$ of the narrow peak. Such a discussion will show that essential features of Lévy statistics were already implicitly used in those arguments although they were not explicitly formulated.

The first estimation [AAK88] of $w(\theta)$ was done in the following way. Since only atoms of momentum p such that $R(p)\,\theta \leq 1$ can remain trapped during the whole interaction time θ, it is natural to define a time-dependent characteristic momentum

p_θ by

$$R(p_\theta)\,\theta = 1 \qquad \text{or, equivalently,} \qquad \tau(p_\theta) = \frac{1}{R(p_\theta)} = \theta \tag{6.1}$$

which gives, using eq. (3.5):

$$p_\theta = p_0 \left(\frac{\tau_0}{\theta}\right)^{1/\alpha}. \tag{6.2}$$

The heuristic argument consisted in conjecturing that p_θ would give the order of magnitude of the half-width $w(\theta)$ of the cooled peak:

$$w(\theta) \simeq p_\theta. \tag{6.3}$$

Numerical solution of the Generalized Optical Bloch Equations (GOBE) for one-dimensional $\sigma^+ - \sigma^-$ laser configurations ($\alpha = 2$) indeed confirmed the $\theta^{-1/2}$ behaviour of the peak half-width predicted by eqs. (6.2) and (6.3), over the limited time range ($\simeq$1500 Γ^{-1}) reachable in a reasonable computer time [AAK89]. The order of magnitude of the prefactor in eq. (6.2) was also confirmed numerically. Two different analytical solutions of the same one-dimensional problem, based on the GOBE, agreed with eq. (6.2) and eq. (6.3) [AlK92, SSY97]. The same $\theta^{-1/2}$-dependence was also observed in a numerical solution of a specific two-dimensional laser configuration [MaA91].

Though well established in specific cases, the above heuristic argument suffers from a basic flaw which limits its generality: it makes the implicit assumption that the atoms in the cooled peak at the end of the interaction time θ did remain trapped for the whole interaction time θ. Obviously, this cannot be strictly true, since the atoms need to perform a random walk to reach the trap, which usually takes a non-negligible time. They enter the trap and they exit it several times. Those in the trap at time θ may have entered the trap the last time a short time τ before θ and their momentum p can be then much larger than p_θ because p is only restricted by the condition that such an atom must remain for a time at least equal to τ (which, in this case, is much smaller than θ). In order to be allowed to neglect the contribution of the atoms that, at time θ, have not been trapped for a very long time, *we must implicitly assume that the total time θ is actually dominated by the duration of a single event* – the trapping time for an atom having its momentum within the peak. We recognize here the unusual behaviour of Lévy statistics, where a single term can determine the behaviour of a Lévy sum. We thus expect from such a discussion that eq. (6.3) will hold approximately true only if the trapping times τ obey a broad distribution with infinite mean.

6.2 Expressions of the momentum distribution and of related quantities

6.2.1 Distribution of the momentum modulus

We first introduce the distribution $\mathcal{P}(p,\theta)$ of the momentum *modulus* p, restricted to the trapping zone $p \leq p_{\rm trap}$. An atom trapped with momentum p at time θ might have reached the p state ($0 \leq p \leq p_{\rm trap}$) at any time t_l ($0 \leq t_l \leq \theta$), provided that it then remained in the trap at least until θ. The 'date' t_l is thus the *last* trapping date, i.e. it satisfies $t_l + \tau \geq \theta$ where τ is the time spent in the p state, which is distributed, conditionally to p, as $P(\tau|p)$. The probability density to reach a p state at time t_l is simply given by $\rho(p)\, S_{\rm R}(t_l)$, where $S_{\rm R}(t_l)$ is the sprinkling distribution calculated in Chapter 5 and $\rho(p) = Dp^{D-1}/p_{\rm trap}^D$ is the probability density (see eq. (3.28)) for an atom entering the trap to have a momentum modulus p (as in Chapter 3, we suppose that $p_{\rm trap} \ll \hbar k$, so that the volume of the trap is reached uniformly). Thus the probability $\mathcal{P}(p,\theta)$ is the sum (over all possible t_l) of the probability $\rho(p) S_{\rm R}(t_l)$ of reaching the trap at time t_l with momentum p, multiplied by the probability $\psi(\theta - t_l|p)$ that the trapping time τ exceeds $\theta - t_l$ for an atom with momentum p:

$$\mathcal{P}(p,\theta) = \rho(p) \int_0^\theta {\rm d}t_l\, S_{\rm R}(t_l)\psi(\theta - t_l|p) \tag{6.4}$$

where

$$\psi(\tau|p) = \int_\tau^\infty {\rm d}\tau' P(\tau'|p). \tag{6.5}$$

Recalling that

$$P(\tau) = \int_0^{p_{\rm trap}} {\rm d}p\, \rho(p) P(\tau|p) \tag{6.6}$$

is the probability that the trapping time within $p_{\rm trap}$ is equal to τ, it is easy to check that, as expected:

$$\int_0^{p_{\rm trap}} {\rm d}p\, \mathcal{P}(p,\theta) = \int_0^\theta {\rm d}t_l\, S_{\rm R}(t_l) \int_{\theta - t_l}^\infty {\rm d}\tau\, P(\tau) = f_{\rm trap}(\theta) \tag{6.7}$$

(see eq. (5.5) and eq. (5.6)).

We shall consider in the following the two models introduced in Section 3.3.1, i.e. a deterministic model where

$$P(\tau|p) = \delta[\tau - \tau(p)] \tag{6.8}$$

and an exponential model where

$$P(\tau|p) = \frac{1}{\tau(p)} \exp\left[-\tau/\tau(p)\right]; \tag{6.9}$$

the two corresponding values of $\psi(\tau|p)$ are:

$$\psi(\tau|p) = Y[\tau(p) - \tau] \tag{6.10}$$

for the deterministic model (Y being the Heaviside function) and

$$\psi(\tau|p) = \exp[-\tau/\tau(p)] \tag{6.11}$$

for the exponential model. According to eq. (3.5), the dependence of $\tau(p)$ on the momentum p is given, in general, by:

$$\tau(p) = \tau_0 \left(\frac{p_0}{p}\right)^{\alpha}. \tag{6.12}$$

Finally, a general result concerning the tails of the momentum distribution can be simply derived from eq. (6.4). For $p \gg p_\theta$, we have $\tau(p) \ll \theta$ according to eq. (6.1). Equations (6.10) and (6.11) then show that $\psi(\theta - t_l|p)$ has non-zero values only if $\theta - t_l \lesssim \tau(p) \ll \theta$, so that only the region $t_l \sim \theta$ will contribute to the integral of eq. (6.4). Since $S_{\mathrm{R}}(t)$ varies more slowly than $\psi(t|p)$, one can write:

$$\mathcal{P}(p,\theta) \underset{p\gg p_\theta}{\simeq} \rho(p) S_{\mathrm{R}}(\theta) \int_0^\infty \mathrm{d}\tau' \psi(\tau'|p) = \rho(p) S_{\mathrm{R}}(\theta) \int_0^\infty \mathrm{d}\tau' \tau' P(\tau'|p) \tag{6.13}$$

where the last equality follows from an integration by parts. By definition, $\tau(p)$ is the average trapping time at momentum p, and hence, we finally get the general result:

$$\mathcal{P}(p,\theta) \underset{p\gg p_\theta}{\simeq} \rho(p) S_{\mathrm{R}}(\theta)\, \tau(p). \tag{6.14}$$

Note that the only dependence on the model is in $S_{\mathrm{R}}(\theta)$ through the quantity τ_{b}, which is equal to τ_{trap} for the deterministic model, and to $\tau_{\mathrm{trap}}[\mu\Gamma(\mu)]^{1/\mu}$ for the exponential model (see eq. (3.33) and eq. (3.34)). We will discuss in Chapter 7 the physical meaning of such a simple expression in terms of a 'quasi-equilibrium' regime.

6.2.2 *Momentum distribution along a given axis*

We suppose that the three-dimensional momentum distribution $\mathcal{P}(\mathbf{p},\theta)$ is spherically symmetric, and we introduce the reduced momentum distribution $\pi(p,\theta)$ such that:

$$\mathcal{P}(p,\theta) = S_D p^{D-1} \pi(p,\theta), \tag{6.15}$$

where $\mathcal{P}(p,\theta)$ is the distribution of the momentum modulus introduced in Section 6.2.1 and where $S_D p^{D-1}$ is the surface of the sphere of radius p in D dimensions

(see eq. (3.27)). In fact, $\pi(p,\theta)$ is the section of the three-dimensional momentum distribution $\mathcal{P}(\mathbf{p},\theta)$ along any axis[1] passing through the origin $\mathbf{p} = \mathbf{0}$. For example,

$$\pi(p,\theta) = \mathcal{P}(p_x = p,\, p_y = 0,\, p_z = 0,\theta). \tag{6.16}$$

Equation (6.4) and eq. (3.26) then give

$$\pi(p,\theta) = \frac{1}{V_D(p_{\rm trap})} \int_0^\theta \mathrm{d}t_l\; S_{\rm R}(t_l)\psi(\theta - t_l|p), \tag{6.17}$$

where $V_D(p_{\rm trap}) = C_D\, p_{\rm trap}^D$ is the volume of a D-dimensional sphere of radius $p_{\rm trap}$ (see eq. (3.24)).

In the tails ($p \gg p_\theta$), a calculation similar to the one leading to eq. (6.14) gives:

$$\pi(p,\theta) \underset{p\gg p_\theta}{\simeq} \frac{1}{V_D(p_{\rm trap})} S_{\rm R}(\theta)\,\tau(p). \tag{6.18}$$

6.2.3 Characterization of the cooled atoms' momentum distribution

From $\pi(p,\theta)$, we can define (by analogy with the rms value for a Gaussian distribution) the $\mathrm{e}^{-1/2}$ *half-width* of the peak of cooled atoms, denoted $w(\theta)$, through:

$$\pi(p = w(\theta),\theta) = \mathrm{e}^{-1/2}\,\pi(p = 0,\theta). \tag{6.19}$$

In order to characterize the momentum distribution of the trapped atoms, it is also useful to introduce the *median* momentum $p_{\rm m}(\theta)$ of the trapped atoms such that:

$$\int_0^{p_{\rm m}} \mathcal{P}(p,\theta)\,\mathrm{d}p = \frac{1}{2} f_{\rm trap}(\theta) = \frac{1}{2}\int_0^{p_{\rm trap}} \mathcal{P}(p,\theta)\,\mathrm{d}p. \tag{6.20}$$

The *height* $h(\theta)$ of the cooled peak is simply defined by

$$h(\theta) = \pi(p = 0,\theta) = \mathcal{P}(\mathbf{p} = \mathbf{0},\theta). \tag{6.21}$$

From eq. (6.17), one obtains:

$$h(\theta) = \frac{1}{V_D(p_{\rm trap})}\int_0^\theta S_{\rm R}(t_l)\,\mathrm{d}t_l \tag{6.22}$$

independently of the shape of $P(\tau|p)$, since for $p = 0$, $\tau(p) = \infty$, so that $\psi(\tau|p = 0) = 1$ (see eqs. (6.10) and (6.11)). (Note again that $S_{\rm R}(t_l)$ depends on the chosen model through $\tau_{\rm b}$.)

[1] Note that $\pi(p,\theta)$ is *not* the probability distribution of p_x which would be obtained by integrating $\mathcal{P}(p_x, p_y, p_z,\theta)$ over p_y and p_z. The dimension of $\pi(p,\theta)$ is $1/p^D$.

Equation (6.22) can be interpreted intuitively: the height of the cooled peak is proportional to the number of atoms that have reached the state $p = 0$ between $t = 0$ and $t = \theta$. Since the probability of entering the trap between t_l and $t_l + \mathrm{d}t$ is equal to $S_{\mathrm{R}}(t_l)\mathrm{d}t_l$, its integral indeed gives the total number of entries in the trap. The factor $1/V_D(p_{\mathrm{trap}})$ is related to the fraction of atoms which fall in the trap at $p = 0$ (where they remain indefinitely) rather than anywhere else in the trap.

The Laplace transform of $h(\theta)$ is

$$\mathcal{L}h(s) = \frac{\mathcal{L}S_{\mathrm{R}}(s)}{sV_D(p_{\mathrm{trap}})}, \tag{6.23}$$

an equation which will be useful later on.

One can also define the *fraction of cooled atoms* $f_{\mathrm{peak}}(\theta)$ as the proportion of atoms of momentum less than one of the above characteristic momentum, for example p_θ:

$$f_{\mathrm{peak}}(\theta) = \int_0^{p_\theta} \mathcal{P}(p,\theta)\,\mathrm{d}p. \tag{6.24}$$

Finally, another important physical quantity is the *phase space density* $\mathcal{D}(\theta)$ in $\mathbf{p} = 0$. In most experiments, one can neglect the increase of the spatial volume occupied by the atoms during the interaction time[2]. This is due to the fact that spatial diffusion is much slower than momentum diffusion. In such a case, the increase of the phase space density exactly reflects the increase of the momentum space density, which is described by the increase of $h(\theta)$.

The quantities $\mathcal{P}(p,\theta)$, $\pi(p,\theta)$, $h(\theta)$ and $f_{\mathrm{peak}}(\theta)$, given by eqs. (6.4), (6.17), (6.22) and (6.24), characterize the momentum distribution. Therefore they cannot depend on the parameter p_{trap} which was introduced only for convenience in intermediate

[2] Note that this is not trivial since Lévy flights can also appear in real space and could lead to anomalously fast diffusion. In fact, as shown here, this is not the case because the long trapping times actually correspond to small velocities.
Let $\Pi(l)$ be the distribution of the jump lengths l in real space between two photon scatterings. If we consider only the jumps of the trapped atoms, $\Pi(l)$ is given by $\Pi(l)\mathrm{d}l = \rho(p)\mathrm{d}p$, where $\rho(p) = Dp^{D-1}/p_{\mathrm{trap}}^D$ is the probability density for an atom entering the trap to have the momentum p. The jump length $l(p)$ for an atom with momentum p is given by the free flight relation $l(p) = p\,\tau(p)/M$ where $\tau(p) = 1/R(p) \propto p^{-\alpha}$ is the duration of the free flight for such an atom. Using such a relation between $l(p)$ and p to calculate $|\mathrm{d}p/\mathrm{d}l|$, we obtain:

$$\Pi(l) = \rho(p)\,|\mathrm{d}p/\mathrm{d}l| \propto \frac{1}{l^{1+D/(\alpha-1)}}. \tag{6.25}$$

One can recognize a broad distribution with a power-law tail described by the exponent $\mu' = D/(\alpha-1)$. We restrict ourselves to the case $\alpha \geq 1$ where long jumps are associated with the region $p \simeq 0$. Quantitatively, for one-dimensional VSCPT with $\theta = 10^5\,\Gamma^{-1}$ and metastable helium atoms, one finds that the spatial expansion due to this Lévy flight process ($\alpha = 2$, $\mu' = 1$) is negligible compared to the expansion due to standard random walk of the untrapped atoms, which is itself negligible compared to the usual size of the cloud of atoms ($\sim$500 μm, see [Bar95]). Therefore, position diffusion can be neglected. Note finally that Lévy flights in position space can also occur in usual (not subrecoil) laser cooling [MEZ96]. Such an anomalous diffusion has been observed for a single ion trapped in an optical lattice [KSW97].

calculations. The appearance of $p_{\rm trap}$ in the above expressions is only formal, since all four expressions involve the product of $1/p_{\rm trap}^{D}$ with some integral of $S_{\rm R}(t)$, which turns out to be proportional to $p_{\rm trap}^{D}$.

It is now straightforward to calculate the momentum distribution and the above related quantities. The given expressions mostly depend on the sprinkling distribution $S_{\rm R}(t)$. The accuracy of the calculations is thus determined by the accuracy of the expression used for $S_{\rm R}(t)$ for large t. Here, the calculations will be carried on to the leading order[3] in t. As a consequence, the results will be exact in the long time limit and approximate for intermediate times. The results depend strongly on the finiteness of $\langle\tau\rangle$ and $\langle\hat{\tau}\rangle$. We shall treat here the general case where $\mu \neq 1$. The case $\mu = 1$ – of some importance in practice – is treated in Appendix C.

6.3 Case of an infinite average trapping time and a finite average recycling time

This case is important in practice: it applies to efficient cooling schemes in which friction provides a fast recycling ($\langle\hat{\tau}\rangle$ finite) while filtering enables the accumulation of a large fraction of trapped atoms ($\langle\tau\rangle$ infinite). We have seen in Chapter 5 that the trapped fraction $f_{\rm trap}(\theta)$ tends to one in this case.

6.3.1 Explicit form of the momentum distribution

We focus here on the momentum distribution $\pi(p,\theta)$ along a given axis and we introduce into eq. (6.17) the leading term in t of the sprinkling distribution $S_{\rm R}(t)$ (see eq. (5.21))

$$S_{\rm R}(t) \simeq \frac{\sin(\pi\mu)}{\pi\,\tau_{\rm b}^{\mu}} t^{\mu-1}.$$

Using p_θ such that $\tau(p_\theta) = \theta$ (see eqs. (6.1) and (6.2)) and changing variables to

$$q = \frac{p}{p_\theta}, \tag{6.26a}$$

$$u = \frac{t_l}{\theta}, \tag{6.26b}$$

one can rewrite eq. (6.17) as:

$$\pi(p = q p_\theta, \theta) = \frac{\sin(\pi\mu)}{\pi\, C_D} \frac{\theta^{\mu}}{\tau_{\rm b}^{\mu}\, p_{\rm trap}^{D}} \int_0^1 {\rm d}u\; u^{\mu-1} \psi(q^{\alpha}(1-u)) \tag{6.27}$$

[3] Except in Chapter 9 where the next order will be needed for optimization purposes.

where $\psi(q^\alpha(1-u))$ is equal to $Y[1-q^\alpha(1-u)]$ for the deterministic model (eq. (6.10)) and to $e^{-q^\alpha(1-u)}$ for the exponential one (eq. (6.11)). Using $\mu = D/\alpha$, $\tau_b^\mu = \mathcal{A}_\mu \tau_{trap}^\mu$ and $t_0 p_0^\alpha = \tau_{trap} p_{trap}^\alpha = \theta p_\theta^\alpha$, we can then transform eq. (6.27) into

$$\pi(p = q p_\theta, \theta) = \frac{\sin(\pi\mu)}{\pi\mu\mathcal{A}_\mu C_D} \frac{1}{p_\theta^D} \mathcal{G}(q) \tag{6.28}$$

where the function $\mathcal{G}(q)$ is equal to:

$$q \leq 1: \qquad \mathcal{G}(q) = 1 \tag{6.29a}$$

$$q \geq 1: \qquad \mathcal{G}(q) = 1 - \left(1 - q^{-\alpha}\right)^\mu \tag{6.29b}$$

for the deterministic model (6.10), and

$$\mathcal{G}(q) = \mu \int_0^1 du\, u^{\mu-1} e^{-(1-u)q^\alpha} \tag{6.30}$$

for the exponential model (6.11)[4]. Note that for both models, we have chosen to impose $\mathcal{G}(0) = 1$, rather than to normalize the integral of $\mathcal{G}$ to the same value. In both cases, $\mathcal{G}(q \to \infty) \simeq \mu q^{-\alpha}$ (in the latter case, only the neighbourhood of $u = 1$ contributes to the integral defining $\mathcal{G}$).

Using the fact that $\mathcal{G}(0) = 1$, expression (6.28) for $\pi(p, \theta)$ can be written in terms of the reduced momentum $q = p/p_\theta$ and the height $h(\theta)$ of the cooled peak as:

$$\pi(p, \theta) = h(\theta)\, \mathcal{G}\left(\frac{p}{p_\theta}\right) = h(\theta)\, \mathcal{G}\left[\frac{p}{p_0}\left(\frac{\theta}{\tau_0}\right)^{1/\alpha}\right] \tag{6.31}$$

with[5]

$$h(\theta) = \frac{\sin(\pi\mu)}{\pi\mu\mathcal{A}_\mu C_D} \frac{1}{p_\theta^D} \propto \theta^\mu. \tag{6.32}$$

The functions $\mathcal{G}(q)$ are drawn in Fig. 6.1 for $\alpha = 2$ and $D = 1$, corresponding to $\mu = 1/2$. The tails of $\mathcal{G}(q)$ vary as $1/(2q^2)$ in agreement with the naive 'ergodic' result $\pi(p, \theta) \propto \tau(p)$, i.e. the population of the p state is proportional to the mean residence time $\tau(p)$ in this state. However, the Lorentzian tails of $\mathcal{G}(q)$ do not imply that $\mathcal{G}(q)$ itself is a Lorentzian. In Fig. 6.2 we compare $\mathcal{G}(q)$ for the exponential model with a Lorentzian having the same normalization and the same tails as $\mathcal{G}(q)$. The important point is that $\mathcal{G}(q)$ is much 'flatter' than the Lorentzian for $q \leq 1$. This is also particularly clear for the deterministic case (see Fig. 6.1)

[4] The expression (6.30) for the exponential model is a confluent hypergeometric function: $\mathcal{G}(q) = M(1, 1+\mu, -q^\alpha)$ (see eq. (13.2.1) in [AbS70]).

[5] An expression of $h(\theta)$ with subleading terms is given in Section 9.4, with an interesting interpretation.

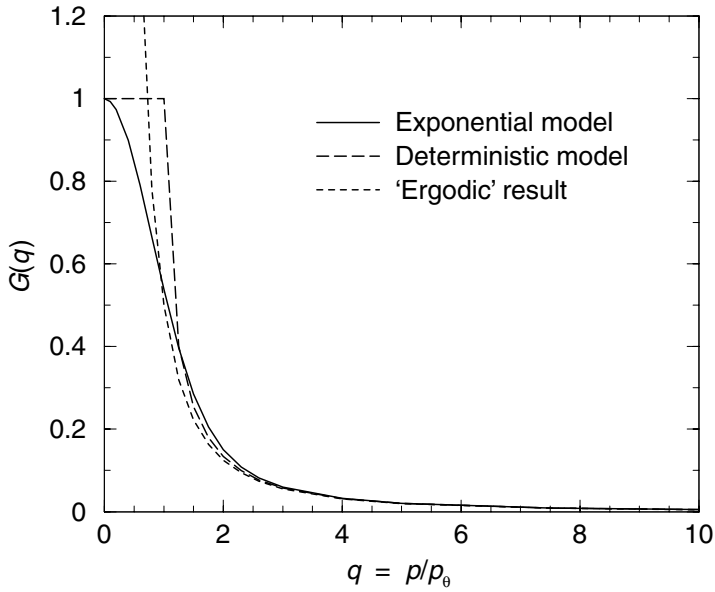

Fig. 6.1. Line shape $\mathcal{G}(q)$ with $q = p/p_\theta$ for $\alpha = 2$ and $D = 1$. The long-dashed curve corresponds to the deterministic model and the solid curve corresponds to the exponential one. The dashed curve represents the 'ergodic' result $1/(2q^2)$ having the same asymptotic behaviour for $q \to \infty$. The characteristic values q_e and q_m defined in Section 6.3.2 are, for the exponential model: $q_e = 0.890\ldots$ and $q_m = 0.798\ldots$.

since $\mathcal{G}(q)$ has a perfectly horizontal plateau for $0 \leq q \leq 1$. We will discuss in the next chapter the physical meaning of such a behaviour and relate it to the non-ergodic character of the cooling process. The difference between $\mathcal{G}$ and a Lorentzian can actually be probed experimentally – see [SLC99] and Section 8.4.3 (Fig. 8.8).

6.3.2 *Important features of the momentum distribution*

There are quite a number of results which can be deduced from expression (6.31).

(i) The momentum distribution $\pi(p, \theta)$ remains self-similar for any θ: $\pi(p, \theta)$ is always given by $\mathcal{G}(q)$ with a proper rescaling of the height and the width.

(ii) The auxiliary parameter p_{trap} no longer appears in expressions (6.31) or (6.32), as expected.

(iii) The momentum $p_{\max}$, which fixes the average recycling time, is also absent from these expressions. This stems from the domination of $S_R(t)$ by trapping times τ whose distribution $P(\tau)$ is broad. Provided that $\langle\hat{\tau}\rangle$ is finite, i.e.

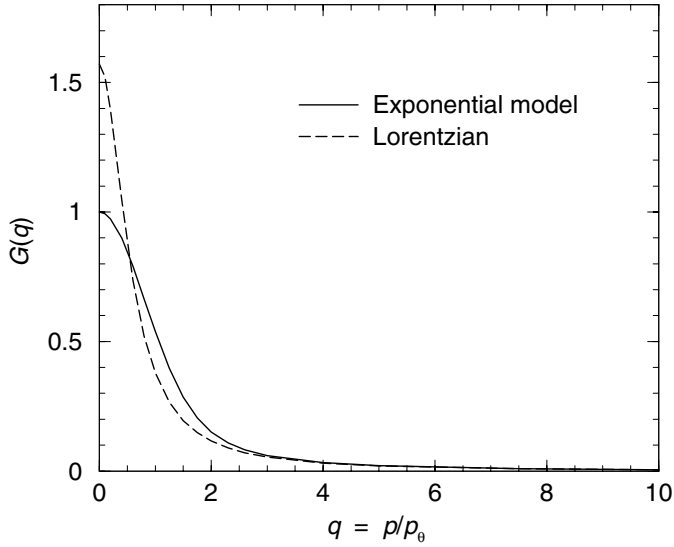

Fig. 6.2. Comparison of $\mathcal{G}(q)$ for the exponential model with a Lorentzian line shape that has the same normalization and the same tails.

provided that $p_{\max}$ is finite, the recycling times $\hat{\tau}$ play no role to leading order when θ is large. This remark also applies to all the quantities related to $\pi(p, \theta)$.

(iv) The height $h(\theta)$ increases with θ, which is *the signature of cooling*. This height increase has a power-law dependence with exponent $\mu = D/\alpha$ determined only by the long tail behaviour of $P(\tau)$.

(v) Since the only p-dependence of $\pi(p, \theta)$ is through the reduced momentum $q = p/p_\theta$, it is clear that the $1/\sqrt{\mathrm{e}}$ half-width $w(\theta)$ is given by

$$w(\theta) = q_{\mathrm{e}} p_\theta \qquad \text{with} \qquad \mathcal{G}(q_{\mathrm{e}}) = \frac{1}{\sqrt{\mathrm{e}}}. \tag{6.33}$$

In eq. (6.33) q_{e} is a numerical factor which depends on μ and α. For the case $\mu = 1/2$, $\alpha = 2$, and in the exponential model, one finds $q_{\mathrm{e}} = 0.890\ldots$. This width thus corresponds, up to a numerical prefactor, to the characteristic momentum p_θ (eq. (6.2)). The same is true for the median momentum $p_{\mathrm{m}}(\theta)$ defined by eq. (6.20), with a different prefactor q_{m}, defined (for $D = 1$) as

$$\int_0^{q_{\mathrm{m}}} \mathrm{d}q\, q^{D-1}\, \mathcal{G}(q) = \frac{1}{2} \int_0^{q_{\mathrm{trap}}} \mathrm{d}q\, q^{D-1}\, \mathcal{G}(q) \tag{6.34}$$

where $q_{\mathrm{trap}} = p_{\mathrm{trap}}/p_\theta$. For the case $\mu = 1/2$, $\alpha = 2$, and still in the

exponential model, one finds $q_{\rm m} = 0.79\ldots$. Thus, at any time θ, most trapped atoms are indeed characterized by a momentum of order p_θ.

(vi) The cooled fraction $f_{\rm peak}(\theta)$ is computed from eq. (6.24) by using eqs. (6.27) and (6.15). The parameter p_θ is then eliminated thanks to eq. (6.2). One finally obtains that $f_{\rm peak}(\theta)$ is a constant (with a value between zero and one), independent of time:

$$f_{\rm peak}(\theta) = \frac{D\sin(\pi\mu)}{\mathcal{A}_\mu \pi\mu}\int_0^1 {\rm d}q\, q^{D-1}\mathcal{G}(q). \tag{6.35}$$

For $D = 1$, $\mu = 1/2$, one finds $f_{\rm peak}(\theta) = 0.59\ldots$ (for the exponential model).

(vii) It is very important to realize that, even if a finite fraction of the trapped atoms have a momentum less than the $e^{-1/2}$ half-width $w(\theta)$, the tails of the distribution are much 'fatter' than for a Maxwellian distribution with the same width. For $p_\theta \ll p \leq p_{\rm trap}$, corresponding to $\tau(p) \ll \theta$, one can use eq. (6.18) which shows that $\pi(p,\theta)$ varies as $S_{\rm R}(\theta)\tau(p)$ for $p \gg p_\theta$. One can also use the asymptotic dependence $\mathcal{G}(q\to\infty) \simeq \mu q^{-\alpha}$ to obtain:

$$\pi(p,\theta) \underset{p\gg p_\theta}{\simeq} \mu h(\theta)\left(\frac{p_\theta}{p}\right)^\alpha \propto \frac{1}{\theta^{1-\mu}p^\alpha}. \tag{6.36}$$

Thus the momentum distribution tails decay with a power-law p-dependence. In particular, for $\alpha = 2$, it decays only as p^{-2}, i.e. as a Lorentzian. The average square momentum is not of order p_θ^2 but rather of order $p_{\rm trap}^D p_\theta^{2-D} \gg p_\theta^2$. We note, however, that in the present case $\mu < 1$, the value of $\pi(p,\theta)$ at a given momentum p decays with θ for $p \gg p_\theta$: the tails therefore shrink. The time evolution of the momentum distribution is shown in Fig. 6.3.

To sum up, the case treated in this section ($\langle\tau\rangle$ infinite and $\langle\hat{\tau}\rangle$ finite) passes all the criteria of efficient cooling: the height of the cooled peak increases with time, its weight is a significant fraction of one and the amplitude of the tails vanishes at large times. However, the shape of the peak is not Maxwell–Boltzmann, but rather has 'fat tails' and a 'flat top'!

6.4 Case of a finite average trapping time and a finite average recycling time

This case is also important in practice: it applies to schemes in which friction provides fast recycling ($\langle\hat{\tau}\rangle$ finite), while filtering is not selective enough to provide an infinite average trapping time ($\langle\tau\rangle$ finite) – which happens when the dimension of space D is larger than the filtering exponent α. In this case, as we have discussed

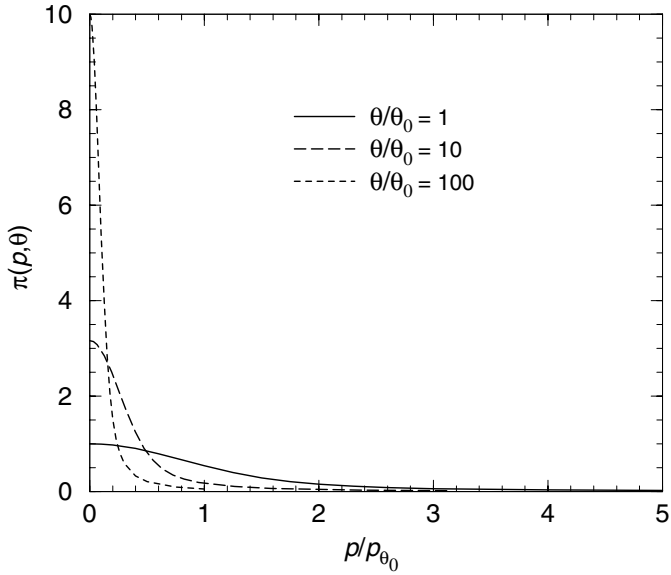

Fig. 6.3. Evolution of the momentum distribution $\pi(p,\theta)$ in the exponential model as θ increases, for $\alpha = 2$ and $D = 1$. The parameter θ_0 is an arbitrary fixed time scale, and p_{θ_0} is the corresponding characteristic momentum. Note that the distribution sharpens with time, while the amplitude of the tails decreases.

in Chapter 5, the trapped fraction $f_{\rm trap}(\theta)$ tends at large times to a constant

$$f_{\rm trap}(\theta) = \frac{\langle\tau\rangle}{\langle\tau\rangle + \langle\hat{\tau}\rangle} = \left(1 + (\mu - 1)\,\frac{p_{\rm max}^D}{p_{\rm trap}^{D-\alpha}\, p_0^\alpha}\right)^{-1}. \tag{6.37}$$

As this constant vanishes for $p_{\rm trap} \to 0$, one might think that subrecoil cooling is inefficient in this case. In fact, the following calculations show unambiguously that subrecoil cooling remains efficient even in this case.

6.4.1 Explicit form of the momentum distribution

The function $S_{\rm R}(t)$ is now given by (see eq. (3.35) and eq. (3.56))[6]:

$$S_{\rm R}(t) \simeq \frac{1}{\langle\tau\rangle + \langle\hat{\tau}\rangle} = \left[\tau_0\left(\frac{\mu}{\mu - 1}\left(\frac{p_0}{p_{\rm trap}}\right)^\alpha + \left(\frac{p_{\rm max}}{p_{\rm trap}}\right)^D\right)\right]^{-1}. \tag{6.38}$$

[6] Eq. (6.38) is exact for the deterministic model. For the exponential model, the first term in the denominator involves a prefactor of order one.

In the limit where $p_{\max} \gg p_{\text{trap}}, p_0$, the above expression simplifies to:

$$S_{\text{R}}(t) \simeq \frac{1}{\langle\hat{\tau}\rangle} = \left[\tau_0 \left(\frac{p_{\max}}{p_{\text{trap}}}\right)^D\right]^{-1}. \tag{6.39}$$

Introducing this formula into eq. (6.17), one finally obtains, after simple integration:

$$\begin{aligned} \pi(p,\theta) &= \frac{1}{C_D p_{\max}^D} \frac{\theta}{\tau_0} \qquad \text{if} \qquad p \le p_\theta \\ &= \frac{1}{C_D p_{\max}^D} \frac{\tau(p)}{\tau_0} \qquad \text{if} \qquad p \ge p_\theta \end{aligned} \tag{6.40}$$

for the deterministic model (6.10), and

$$\pi(p,\theta) = \frac{1}{C_D p_{\max}^D} \frac{\tau(p)}{\tau_0} \left[1 - \exp\left(-\frac{\theta}{\tau(p)}\right)\right] \tag{6.41}$$

for the exponential model (6.11).

These momentum distributions can also be written in a simple scaling form similar to eq. (6.31):

$$\pi(p,\theta) = h(\theta)\, \widetilde{\mathcal{G}}\left(\frac{p}{p_\theta}\right) = h(\theta)\, \widetilde{\mathcal{G}}\left[\frac{p}{p_0}\left(\frac{\theta}{\tau_0}\right)^{1/\alpha}\right] \tag{6.42}$$

with

$$h(\theta) = \frac{1}{C_D\, p_{\max}^D} \frac{\theta}{\tau_0}. \tag{6.43}$$

For the deterministic model, the function $\widetilde{\mathcal{G}}(q)$ is

$$q \le 1: \qquad \widetilde{\mathcal{G}}(q) = 1, \tag{6.44a}$$

$$q \ge 1: \qquad \widetilde{\mathcal{G}}(q) = q^{-\alpha}. \tag{6.44b}$$

For the exponential model, it becomes

$$\widetilde{\mathcal{G}}(q) = q^{-\alpha}\left[1 - \exp(-q^\alpha)\right]. \tag{6.45}$$

Note that $\widetilde{\mathcal{G}}(0) = 1$ and that $\widetilde{\mathcal{G}}(q \to \infty) \simeq q^{-\alpha}$ for both models. The functions $\widetilde{\mathcal{G}}(q)$ are drawn in Fig. 6.4 for $\alpha = 2$ and $D = 3$, corresponding to $\mu = 3/2$. As in the previous section, the distribution $\pi(p,\theta)$ still presents a plateau-like region for $p \le p_\theta$.

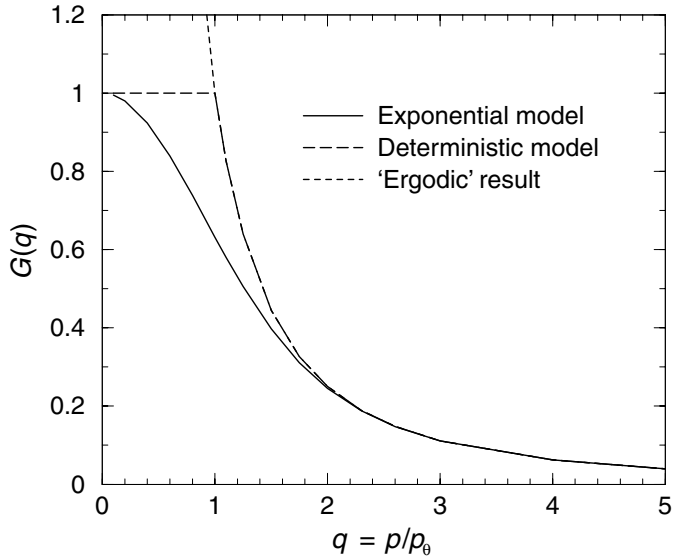

Fig. 6.4. Line shape $\widetilde{\mathcal{G}}(q)$, with $q = p/p_\theta$, for $\alpha = 2$ and $D = 3$. The long-dashed curve corresponds to the deterministic model, the solid curve to the exponential one, and the dashed curve to the 'ergodic' result $\widetilde{\mathcal{G}}(q) \propto 1/(2q^2)$ having the same behaviour as the previous curves for $q \to \infty$. The value of q_e is now 1.048, while the median momentum q_m now depends on p_{trap}.

6.4.2 Important features of the momentum distribution

We point out now a few important features of the momentum distribution.

(i) The curve $\pi(p, \theta)$ is still self-similar for any θ.

(ii) The auxiliary parameter p_{trap} is absent from the expression for $\pi(p, \theta)$.

(iii) Contrary to what happens for the case $\mu < 1$, the momentum p_{max} (which determines the average recycling time) now appears explicitly in eqs. (6.40) and (6.41). This reflects the fact that the trapping events are no longer predominant.

(iv) The height $h(\theta)$ of the peak of cooled atoms, given by eq. (6.43), increases linearly with θ. In this sense, *there is still a real cooling*. A similar increase is predicted for the phase space density.

(v) The $e^{-1/2}$ half-width q_e of $\widetilde{\mathcal{G}}(q)$ is of the order of unity, so that the $e^{-1/2}$ half-width $w(\theta) = q_e p_\theta$ of the momentum distribution $\pi(p, \theta)$ is still of the order of p_θ. However, since $\mu > 1$ is equivalent to $\alpha < D$, the integral over p of $\rho(p)\pi(p, \theta)$ is now dominated by *large* p values. The median momentum

is thus given, when $p_\theta \ll p_{\rm trap}$, by:

$$p_{\rm m} = \frac{1}{2^{1/(D-\alpha)}}\, p_{\rm trap}. \tag{6.46}$$

Thus, the trapped atoms are characterized in this case by a momentum of order $p_{\rm trap} \gg p_\theta$: most trapped atoms reside on the 'border' of the trap.

(vi) The expression for the cooled fraction now reads, after changing variables to $q = p/p_\theta$:

$$f_{\rm peak}(\theta) = Dh(\theta) p_\theta^D \int_0^1 {\rm d}q\, q^{D-1} \widetilde{\mathcal{G}}(q). \tag{6.47}$$

Using the fact that $h(\theta) \propto \theta$ and that $p_\theta \propto \theta^{-1/\alpha}$, one finally finds that $f_{\rm peak}(\theta) \propto \theta^{1-\mu}$. Since now $\mu > 1$, $f_{\rm peak}(\theta)$ decreases to 0 when $\theta \to \infty$.

(vii) It clearly appears in eq. (6.40), and also in eq. (6.41), that, for $p \gg p_\theta$, $\pi(p, \theta)$ no longer depends on θ and has a p-dependence identical to that of $\tau(p)$. Thus, as shown in Fig. 6.5, the tails of the momentum distribution reach a steady-state when θ increases. They decrease with p as a power-law $p^{-\alpha}$ (for $\alpha = 2$, the tails have a Lorentzian shape). In fact, the momentum distribution (6.40) or (6.41) remains unchanged in the tails when θ increases. Note, however, that the value p_θ of the truncation decreases when θ increases.

To sum up, the case of finite $\langle\tau\rangle$ and finite $\langle\hat{\tau}\rangle$ presents a rather subtle cooling behaviour: the cooled fraction tends to zero at large times – the trapped atoms accumulate mostly in the tails of the peak, but there is still a clear cooling effect, since the peak height and therefore the momentum and the phase space densities increase significantly.

6.5 Cases with an infinite average recycling time

The cases with $\langle\hat{\tau}\rangle$ infinite are not very favourable for cooling. Even though it seems almost always possible experimentally to make $\langle\hat{\tau}\rangle$ finite, these cases are important because several precise one-dimensional σ_+/σ_- VSCPT experiments, as well as numerical simulations, have been done with and correspond to infinite $\langle\hat{\tau}\rangle$. Moreover, one special case with infinite $\langle\hat{\tau}\rangle$ presents a significant new feature. We therefore briefly present here the various situations with infinite $\langle\hat{\tau}\rangle$ discussing in detail only the special case that brings a novel feature.

- If $\mu < \hat{\mu}$ (< 1), the sprinkling distribution $S_{\rm R}(t)$ is, at first order, exactly the same as in Section 6.3, and so is the probability distribution $P(\tau)$ of the trapping times. Thus, one obtains exactly the same features for the momentum distribution as in Section 6.3, where the trapping periods also dominate.

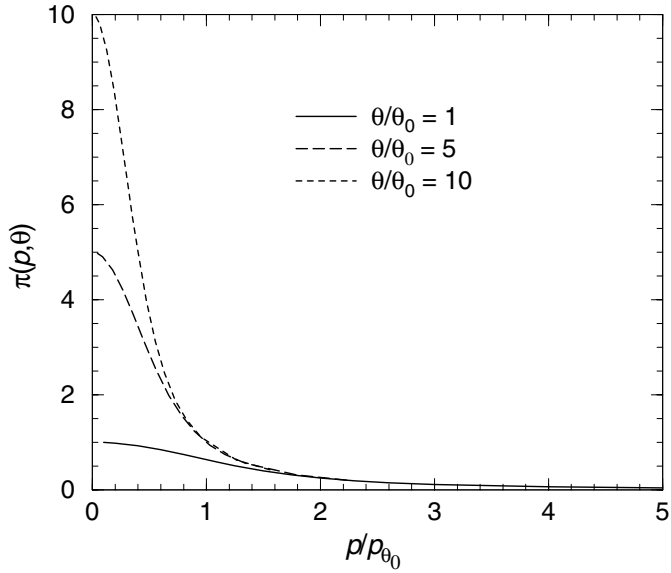

Fig. 6.5. Evolution of the momentum distribution $\pi(p,\theta)$ in the exponential model as θ increases for $\alpha = 2$, $D = 3$ ($\langle\tau\rangle$ and $\langle\hat{\tau}\rangle$ finite). The parameter θ_0 is an arbitrary fixed time scale. Note that while the height of the distribution increases with time, its tails reach a stationary (time independent) state (compare with Fig. 6.3). Note also that since $f_{\text{peak}}(\theta)$ is the integral from 0 to $p_\theta = p_0(\tau_0/\theta)^{1/\alpha}$ of the product of $\pi(p,\theta)$ and p^{D-1}, the fraction of cooled atoms goes to zero for large θ.

- If $\mu = \hat{\mu}$ (< 1), the first term of the Laplace transform of the sprinkling distribution $S_{\text{R}}(t)$ is the same as in the case $\mu < 1 < \hat{\mu}$ (compare eq. (5.28) and eq. (5.21)), except for the numerical prefactor. Thus, the results of Section 6.3 on the momentum distribution $\pi(p,\theta)$ still hold, except that the numerical prefactor of $\pi(p,\theta)$ will be smaller due to the finite proportion of time spent by the atoms in the recycling zone. This case applies to one-dimensional σ_+/σ_- VSCPT cooling in the regime of intermediate times for which the Doppler effect is negligible (see Sections 8.3.2, 8.4 and A.1.1.5 (p. 153)).
- If $\hat{\mu} < \mu$ (< 1), the behaviour of the cooling becomes slightly different from the previously treated cases, but the derivations are similar. This special case applies to one-dimensional σ_+/σ_- VSCPT in the long time regime for which the Doppler effect slows down the atomic diffusion at large p. The sprinkling distribution $S_{\text{R}}(t)$ is now dominated by recycling times and we can write, in analogy with eq. (5.21),

$$S_{\text{R}}(t) = \frac{\sin(\pi\hat{\mu})}{\pi}\hat{\tau}_{\text{b}}^{-\hat{\mu}}t^{\hat{\mu}-1} + \cdots . \tag{6.48}$$

Proceeding as in Section 6.3.1, we obtain

$$\pi(p,\theta) = h(\theta)\,\hat{\mathcal{G}}\left(\frac{p}{p_\theta}\right) = h(\theta)\,\hat{\mathcal{G}}\left[\frac{p}{p_0}\left(\frac{\theta}{\tau_0}\right)^{1/\alpha}\right], \tag{6.49}$$

where the height $h(\theta)$ of the peak is

$$h(\theta) = \frac{\sin(\pi\hat{\mu})}{\pi\hat{\mu}C_D p_{\text{trap}}^D \hat{\tau}_{\text{b}}^{\hat{\mu}}}\,\theta^{\hat{\mu}} \tag{6.50}$$

and where the shape $\hat{\mathcal{G}}(q)$ is

$$q \le 1: \qquad \hat{\mathcal{G}}(q) = 1 \tag{6.51a}$$

$$q \ge 1: \qquad \hat{\mathcal{G}}(q) = 1 - \left(1 - q^{-\alpha}\right)^{\hat{\mu}} \tag{6.51b}$$

for the deterministic model (6.10), and

$$\hat{\mathcal{G}}(q) = \hat{\mu}\int_0^1 \mathrm{d}u\; u^{\hat{\mu}-1}\mathrm{e}^{-(1-u)q^\alpha} \tag{6.52}$$

for the exponential model (6.11).

Interesting features of the momentum distribution in this case are as follows.

(i) The curve $\pi(p,\theta)$ is self-similar for any θ.

(ii) The auxiliary parameter p_{trap} is still present in $h(\theta)$ because, to maintain the generality of the treatment, we have not replaced $\hat{\tau}_{\text{b}}$ by is explicit expression containing p_{trap}. If this was done, p_{trap} would disappear.

(iii) There is no momentum $p_{\max}$ in this problem.

(iv) The height $h(\theta)$ still increases in this case, in spite of the domination of recycling times over trapping times. *There is thus still real cooling.* Of course, the increase is slower than when trapping times dominate, i.e. when $\mu < \hat{\mu}$.

(v) The $\mathrm{e}^{-1/2}$ half-width q_{e} of $\hat{\mathcal{G}}(q)$ and the median q_{m} are of the order of unity. This indicates that the (few) trapped atoms are characterized by a momentum of order p_θ: most of them are in the cooled peak.

(vi) The cooled fraction $f_{\text{peak}}(\theta)$ tends to zero as $\theta \to \infty$.

(vii) The tails of the momentum distribution $\pi(p,\theta)$ vary as $p^{-\alpha}$ for $p \gg p_\theta$, as in previously treated cases. On the other hand, for small momenta, we now have $\hat{\mathcal{G}}(q) \underset{q\to 0}{=} 1 - q^\alpha/(1+\hat{\mu})$ (exponential model), while we had $\mathcal{G}(q) \underset{q\to 0}{=} 1 - q^\alpha/(1+\mu)$ in all previously treated cases. Thus, the shape of the momentum distribution *in the vicinity of* $p = 0$ now depends on $\hat{\mu}$, i.e.

it depends on the the jump rate *far away from* $p = 0$. This new feature is a remarkable sign of non-ergodicity (see Section 7.5.1).

To sum up, when $\hat{\mu} < \mu < 1$, even though the cooled fraction tends to zero at large times, there is still a clear cooling effect.

- The case $\hat{\mu} < 1$ (infinite $\langle \hat{\tau} \rangle$) and $\mu > 1$ (finite $\langle \tau \rangle$) is clearly very unfavourable: a vanishingly small fraction of atoms is in the trap, and most of them are near the border p_{trap}.

6.6 Overview of main results

In this chapter, we have derived the momentum distributions of the trapped atoms and expressed them into *scaling forms* $\mathcal{G}(q = p/p_\theta)$ that are time invariant and depend only on μ and α. All cases in which μ and $\hat{\mu}$ are different from one have been treated (the case $\mu = 1$ is treated in Appendix C). Let us concentrate here on the two most favourable cases corresponding to $\langle \hat{\tau} \rangle$ finite and $\langle \tau \rangle$ either infinite ($\mu < 1$) or finite ($\mu > 1$) (see Sections 6.3 and 6.4). The most important results are gathered in table 6.1.

Table 6.1. *Momentum distribution properties: p and θ dependence in the case where $\langle \hat{\tau} \rangle$ is finite, while $\langle \tau \rangle$ is either infinite ($\mu \leq 1$) or finite ($\mu > 1$).*

	$\mu < 1$	$\mu = 1$	$\mu > 1$
Height $h(\theta)$	θ^{μ}	$\theta / \log \theta$	θ
Half-width $w(\theta)$	$\theta^{-1/\alpha}$	$\theta^{-1/\alpha}$	$\theta^{-1/\alpha}$
Median p_{m}	$\simeq p_\theta \propto \theta^{-1/\alpha}$	$\simeq \sqrt{p_\theta p_{\text{trap}}} \propto \theta^{-1/2\alpha}$	$\simeq p_{\text{trap}} \propto \theta^0$
Cooled fraction $f_{\text{peak}}(\theta)$	1	$1 - \mathcal{O}((\log \theta)^{-1})$	$\theta^{1-\mu}$
Tails $\pi(p \gg p_\theta, \theta)$	$(p^\alpha \theta^{1-\mu})^{-1}$	$(p^\alpha \log \theta)^{-1}$	$(p^\alpha \theta^0)^{-1}$

In both cases ($\mu < 1$ and $\mu > 1$), the following common features were demonstrated. The height $h(\theta)$ of the cooled peak increases with θ, *which is the signature of cooling*. The half-width $w(\theta)$ of the cooled peak is proportional to p_θ. It decreases with θ as $\theta^{-1/\alpha}$ independently of the dimensionality D. The tails of the momentum distribution decay as $1/p^\alpha$.

Apart from these common features, there are important differences between the two cases $\mu < 1$ and $\mu > 1$. The parameter $p_{\max}$ does not appear in any of the characteristic momenta for $\mu < 1$, whereas it explicitly appears for $\mu > 1$ in prefactors not given in table 6.1. The cooled fraction $f_{\text{peak}}(\theta)$ tends to a constant for $\mu < 1$ whereas it decays as $1/\theta^{\mu-1}$ when θ increases for $\mu > 1$. The median momentum p_{m} is, up to a numerical prefactor, equal to p_θ when $\mu < 1$ and to p_{trap} when $\mu > 1$. Finally, the tails of the momentum distribution decrease at large times (as $1/\theta^{1-\mu}$) when $\mu < 1$, whereas they tend to a stationary value when $\mu > 1$.

We will discuss the physical content of these results in the next chapter.